

## Optical signatures of nitrogen acceptors in ZnO

S. Lautenschlaeger, S. Eisermann, G. Haas, E. A. Zolnowski, M. N. Hofmann, A. Laufer, M. Pinnisch, and B. K. Meyer  
*I. Physikalisches Institut, Justus-Liebig-University Gießen, Heinrich Buff-Ring-16, 35392 Gießen, Germany*

M. R. Wagner, J. S. Reparaz, G. Callsen, and A. Hoffmann  
*Institute of Solid State Physics, Technical University Berlin, Hardenbergstrasse 36, 10623 Berlin, Germany*

A. Chernikov, S. Chatterjee, V. Bornwasser, and M. Koch  
*Faculty of Physics and Materials Sciences Center, Philipps University Marburg, Renthof 5, 35032 Marburg, Germany*  
 (Received 20 November 2011; published 21 June 2012)

We report on the optical properties of nitrogen acceptor-doped ZnO epilayers in the medium and high doping regimes using temperature and excitation power-dependent, as well as time-resolved photoluminescence experiments. The epilayers were doped with ammonia during homoepitaxial growth on ZnO single-crystal substrates with different surface polarities. Significant differences in the optical characteristics of the epilayers are observed between growth on nonpolar *a*-plane, polar *c*-plane Zn-face substrates and polar *c*-plane O-face substrates, which demonstrates different incorporation of the nitrogen acceptor depending on the substrate polarity. The incorporation of nitrogen into the ZnO films ranges between  $10^{19}$  and  $10^{21}$  cm<sup>-3</sup> as determined by secondary ion mass spectrometry. Within this doping range the samples change from lightly compensated to highly doped compensated. We discuss the unique photoluminescence features of nitrogen-doped ZnO epilayers within the concept of shallow donor-acceptor-pair recombinations and at the highest doping level by the appearance of potential fluctuations.

DOI: [10.1103/PhysRevB.85.235204](https://doi.org/10.1103/PhysRevB.85.235204)

PACS number(s): 61.72.uj, 78.55.Et, 77.55.hf

### I. INTRODUCTION

The doping of semiconductors with donors and acceptors is typically accompanied by significant changes in the optical properties with respect to intrinsic materials. In the ideal case of impurity- and defect-free material, the free exciton emission usually represents the dominant radiative recombination process. Increasing the doping level leads to the localization of free excitons at impurity sites which are commonly known as donor or acceptor bound excitons. The bound exciton recombinations usually dominate the optical spectra due to the giant oscillator strength of these states which is caused by their high spatial localization.<sup>1</sup> At higher donor and acceptor doping levels the radiative recombination between the donor electrons and acceptor holes gradually becomes the dominant process. The case of ZnO is particularly interesting in this matter since effective *p*-type doping represents a challenge while *n*-type doping naturally occurs even in the purest samples due to residual impurities and native defects.<sup>2-4</sup> Despite the fact that many reports on *p*-type conductivity in ZnO were published in recent years, a systematic investigation of the influence of *p*-type doping on the optical properties is still missing. Several studies on acceptor doping in ZnO rely exclusively on electrical measurements to claim *p*-type conductivity.<sup>5-7</sup> However, this approach does not provide direct proof of *p*-type conductivity since, e.g., the presence of extended defects and large lattice mismatch of epilayer and substrate can induce an inhomogeneously distributed conductivity in the ZnO films which might lead to an erroneous determination of the doping type.<sup>8-10</sup> Furthermore, even in the best heteroepitaxially and homoepitaxially grown samples defect-related emission lines between 3.31 and 3.35 eV caused by structural disorder (stacking faults, dislocations) are present.<sup>11,12</sup> These transitions can misleadingly be interpreted as recombinations of acceptor

bound excitons ( $A^0X$ ) induced by acceptor doping. However, Schirra *et al.*<sup>11</sup> convincingly demonstrated the dominant role of stacking faults in acceptor-doped ZnO, thereby explaining why so many (potential) acceptor dopants (N, As, P, Sb) contribute to the same free-to-bound recombination ( $e,A$ ) at 3.31 eV while the epilayers still remain *n* type. Furthermore, Wagner *et al.*<sup>12</sup> recently showed that a variety of potential candidates for  $A^0X$  emission lines between 3.33 and 3.35 eV originate in fact from excitons bound to extended structural defects ( $Y$  lines) which introduce deep donor complexes in ZnO. The optical recombinations close to the band edge are thus exclusively caused by ionized and neutral donor bound excitons ( $DX$ ), whereas acceptor bound excitons ( $A^0X$ )—despite several claims in the literature<sup>13,14</sup>—could not doubtlessly be identified so far by, e.g., reliable magneto-optical data. Increasing the acceptor doping decreases the photoluminescence (PL) intensity of the neutral donor bound excitons ( $D^0X$ ) in favor of ionized ones ( $D^+X$ ) before donor-acceptor pair (DAP) recombinations dominate the optical recombination spectra. While this is a common feature for most III-V (GaAs, InP, GaN) and II-VI (CdTe, ZnSe) semiconductors, it has still not been demonstrated for ZnO. Thus, it is our purpose to establish a better understanding of the optical properties of highly N-acceptor-doped ZnO homoepitaxial films using ammonia as the nitrogen source.

The PL properties of nitrogen-doped ZnO have already been investigated by several groups. A broad variety of growth methods such as ion implantation,<sup>15-19</sup> molecular beam epitaxy (MBE),<sup>20-22</sup> chemical vapor deposition (CVD),<sup>18, 23-26</sup> and pulsed-laser deposition (PLD)<sup>27-30</sup> were employed to fabricate the doped samples. The optical spectra of most of the investigated samples exhibit three common features: (i) a dominating  $DX$  recombination (regarding peak intensity),

(ii) a DAP band around 3.24 eV, and (iii) the emission of structural defect bound excitons.<sup>12</sup> This indicates on the one hand that the prevailing *n*-type conductivity [caused by residual donors such as aluminum ( $\text{Al}_{\text{Zn}}$ ), gallium ( $\text{Ga}_{\text{Zn}}$ ), or zinc interstitials ( $\text{Zn}_i$ )] still persists; on the other hand it proves that structural disorder (stacking faults, dislocations, etc.) can severely influence the optical quality of the films. Regarding the DAP band arising from the incorporation of nitrogen, different energetic positions were reported throughout the literature. Although the DAP bands between 3.18 and 3.25 eV (Refs. 15,23,26,27,31,32) were reported to originate from nitrogen acceptors, systematic studies for samples with high nitrogen concentrations ( $>1 \times 10^{20} \text{ cm}^{-3}$ ) have not been presented so far. Such high nitrogen concentrations in ZnO epilayers are rather hard to achieve due to limitations of conventional growth processes. Ion implantation appears to be a suitable growth technique to reach high nitrogen concentrations, but simultaneously induces tremendous damage of the crystalline structure of the host crystal.

In this report we investigate the optical characteristics of highly N-doped ZnO epilayers using ammonia as the nitrogen source. The influence of the polarity on the nitrogen incorporation and optical characteristics is studied for homoepitaxial grown epilayers on different polar and nonpolar faces of ZnO substrates. In order to overcome the low solubility of nitrogen at high growth temperatures we developed a low-temperature CVD process that enables us to incorporate nitrogen up to concentrations of  $1 \times 10^{21} \text{ cm}^{-3}$  in ZnO. The optical properties of the nitrogen-doped epilayers are systematically investigated as a function of the excitation power and temperature, as well as by using time-resolved spectroscopy. Finally, we show that all the optical investigations are in good agreement with the classical picture of successful acceptor incorporation.

## II. EXPERIMENTAL DETAILS

The nitrogen-doped ZnO films have been grown in a CVD process using only metallic zinc,  $\text{NO}_2$ , and  $\text{NH}_3$  as precursors. The reactor pressure and flow of the transport gas (argon) were kept constant for all growth runs. The samples were grown in systematic growth runs with varying growth temperature and dopant flow. Polar *c*-plane (O face and Zn face), and nonpolar *a*-plane ZnO substrates were used to investigate the influence of the polarity of the substrate on the nitrogen incorporation in the films. The N concentration of each ZnO film was determined using a commercial Cameca-Riber secondary ion mass spectroscopy (SIMS) setup with  $\text{Cs}^+$  as primary ions. The conversion between the measured ion counts and the atomic concentrations was achieved by using implantation standards.

The steady-state PL spectra were recorded using the 325-nm laser line of a HeCd laser as excitation source. For the power-dependent measurements the laser beam was focused onto the samples using a microlens while the excitation power density was varied from  $1 \text{ kW cm}^{-2}$  to  $10 \text{ MW cm}^{-2}$ . For the time-resolved photoluminescence (TRPL) experiments we used a diode-pumped titanium-sapphire laser in combination with a frequency tripler as excitation source. The pulse length and repetition rate were 100 fs and 80 MHz, respectively. The samples were placed in a He bath cryostat which allowed temperature control, and the PL transients were recorded using

a standard streak camera with a maximum temporal resolution of  $<1 \text{ ps}$ .

## III. EXPERIMENTAL RESULTS

### A. Nitrogen incorporation

Figure 1 shows the nitrogen concentrations of a series of samples grown on nonpolar *a*-plane substrates at different temperatures as determined by SIMS measurements. From earlier investigations we know that the incorporation of unwanted shallow donors during the CVD process is reduced when using either *a*-plane or *c*-plane Zn-face crystal orientations as compared to O-face ZnO substrates.<sup>33,34</sup> This is reflected in superior optical quality and reduced residual strain in the Zn-face epilayers.<sup>35</sup> Furthermore, it was shown that the incorporation of nitrogen is higher on the Zn-face substrates compared to the O-face substrates.<sup>36</sup> For the *a*-plane orientation, the efficiency of the nitrogen incorporation is found to be comparable to that of the *c*-plane Zn face. Since the nitrogen incorporation strongly depends on the growth temperature we performed growth runs with substrate temperatures between  $200^\circ\text{C}$  and  $600^\circ\text{C}$ . For high growth temperatures above  $550^\circ\text{C}$  a two-dimensional (2D) growth mode was achieved with a FWHM of the in-plane rocking curve of less than 100 arc sec which corresponds to the resolution limit of the used x-ray diffraction machine. In the midtemperature region of  $550^\circ\text{C}$  to  $350^\circ\text{C}$  the resulting epilayers showed an increased FWHM of 200–500 arc sec. Within this temperature range a transition from a purely 2D-growth mode towards a three-dimensional-growth mode occurs. In the case of the low-temperature, high-dopant-flow growth runs we achieved a mixed growth mode resulting in *c*-axis orientated epilayers with grain sizes of around  $2\text{--}5 \mu\text{m}$ . For substrate temperatures of  $250^\circ\text{C}$  which were applied to drive the nitrogen solubility limit above  $10^{21} \text{ cm}^{-3}$ , the FWHM reaches values of 1000 arc sec while the layers are still exclusively *c*-axis orientated. Despite the fact that the optimal growth temperature for ZnO in the applied CVD reactor is

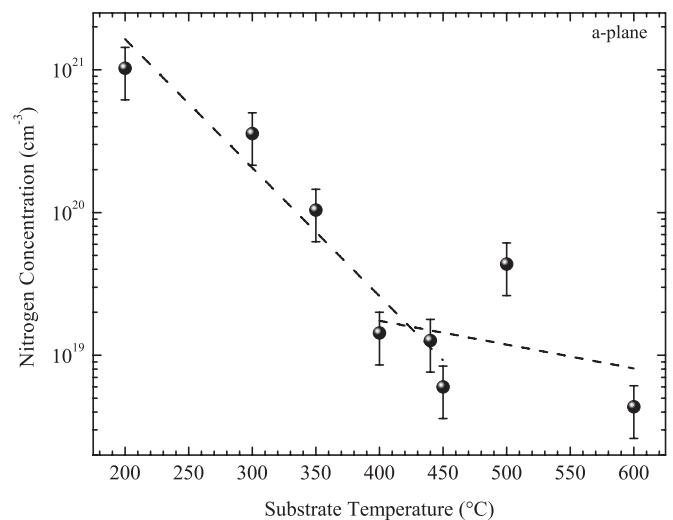


FIG. 1. Nitrogen concentrations of *a*-plane grown ZnO:N epilayers with constant dopant flow for substrate temperatures between  $200^\circ\text{C}$  and  $600^\circ\text{C}$ .

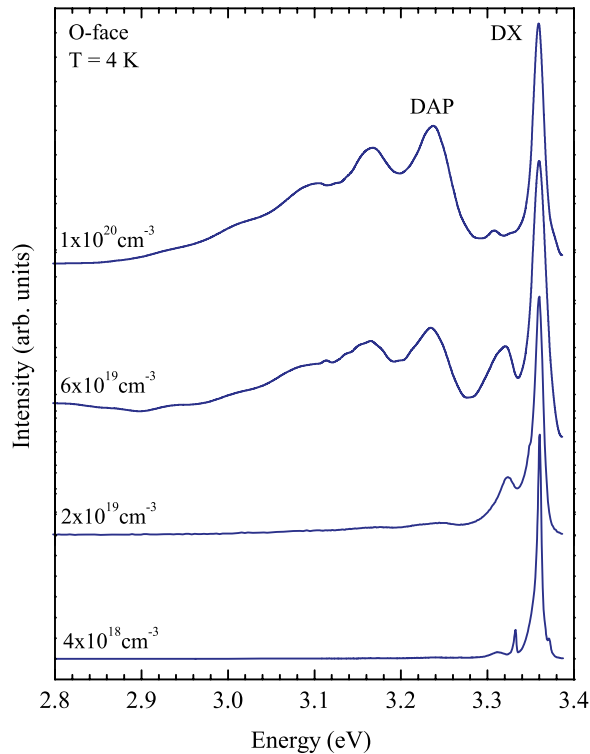


FIG. 2. (Color online) PL of ZnO:N epilayers on O-face *c*-plane substrates with increasing nitrogen concentration measured at  $T = 4$  K.

between  $600^\circ\text{C}$  and  $700^\circ\text{C}$ , lower growth temperatures had to be used in order to incorporate nitrogen with concentrations of more than  $10^{17}\text{ cm}^{-3}$ . The SIMS measurements in Fig. 1 provide a clue for the temperature range which is required to overcome the background donor concentration of about  $1 \times 10^{17}\text{ cm}^{-3}$ . According to the acceptor-complex model<sup>37</sup> the nitrogen concentration that must be used to overcompensate the residual donors ranges between  $10^{19}\text{ cm}^{-3}$  and  $10^{20}\text{ cm}^{-3}$ . Based on the SIMS results these N concentrations can only be achieved for growth temperatures below  $400^\circ\text{C}$ . Consequently, the temperature region for the epilayer growth was kept between  $300^\circ\text{C}$  and  $375^\circ\text{C}$  using the ammonia flow to tune the dopant incorporation.

### B. Steady-state PL

Figure 2 shows the PL spectra of nitrogen-doped ZnO epilayers grown on the *c*-plane O face of ZnO substrates. Depending on the nitrogen concentration a pronounced DAP band around 3.24 eV is observed. This transition has been assigned to a shallow donor to shallow acceptor transition with an acceptor binding energy of around 160 meV and donor binding energies between 52 and 56 meV depending on whether Al or Ga donors are involved.<sup>38,39</sup> As shown in Fig. 2, the intensity of the DAP band relative to that of the DX emission around 3.36 eV systematically rises with increasing nitrogen content in the films. However, the intensity of the DAP band never exceeds that of the DX arising mainly from Al impurities. From the SIMS measurements we determine the Al concentration within the layers to about  $1 \times 10^{17}\text{ cm}^{-3}$ . By contrast, the epilayers grown on *c*-plane Zn-face substrates and

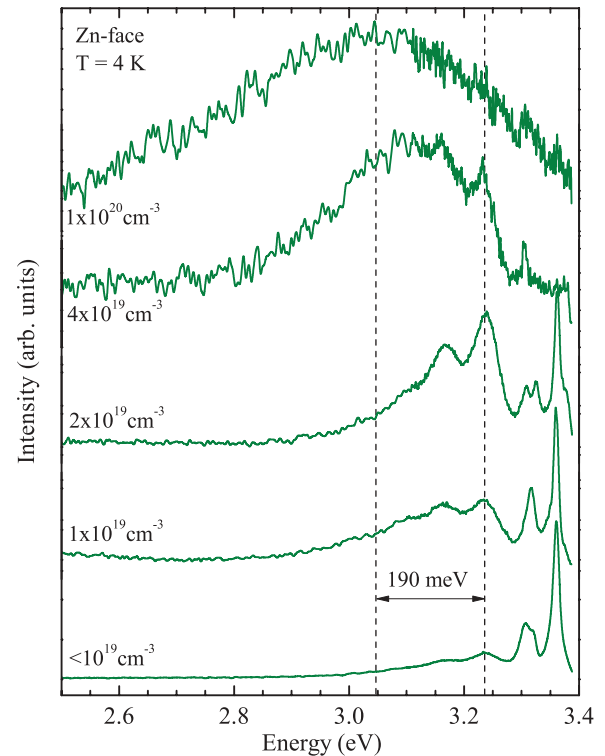


FIG. 3. (Color online) PL of ZnO:N epilayers on Zn-face *c*-plane substrates with increasing nitrogen concentration measured at  $T = 4$  K.

*a*-plane ZnO substrates exhibit a very different PL behavior. The low-temperature PL spectra of the Zn-face samples are shown in Fig. 3 with increasing nitrogen concentrations from  $10^{19}$  to  $10^{20}\text{ cm}^{-3}$ . The spectra show more significant changes if compared to the case of the *c*-plane O-face samples in Fig. 2. The DX intensity gradually diminishes with increasing nitrogen concentration and vanishes completely in the highly doped samples. In addition, a pronounced DAP band is observed for the lowest doping concentration. Finally, with increasing nitrogen concentration the DAP band progressively broadens and shifts towards lower energies. At the highest doping level the DAP band is located around 3.05 eV, i.e., 190 meV deeper than the usual DAP position at around 3.24 eV. This behavior, while newly reported in ZnO, was already observed in many II-VI and III-V semiconductors with high levels of compensation such as ZnSe,<sup>40</sup> GaAs,<sup>41</sup> and GaN,<sup>42</sup> and was successfully explained by Shklovskii and Efros<sup>43</sup> by assuming a fluctuating band structure arising from the interaction of free carriers (here assumed to be holes) with the electric field caused by high amounts of ionized donors and acceptors (fluctuating potentials).

In Fig. 4, we show the ratio between the integrated intensity of the DAP band ( $I_{\text{DAP}}$ ) and the DX recombination ( $I_{\text{DX}}$ ) as function of the total nitrogen concentration for *c*-plane Zn- and O-face samples. This ratio reflects the change in the donor and acceptor concentrations  $N_D$  and  $N_A$ , respectively, and is proportional to  $N_D - N_A$  ( $N_A - N_D$ ) for *n*-type (*p*-type) materials.<sup>44</sup> The results for the *a*-plane epilayer are similar to those of the *c*-plane Zn face shown in Fig. 4. The different slopes for the two different faces indicate that the intensity increase of the DAP band for the Zn-face layers is at least

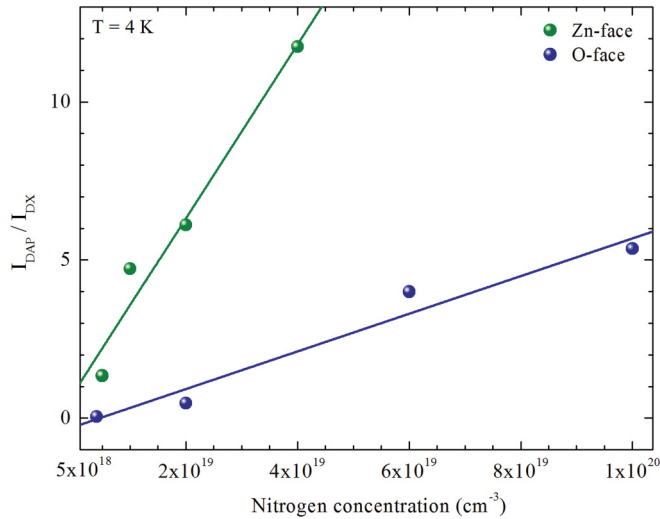


FIG. 4. (Color online) Ratio of the DAP to donor bound exciton luminescence ( $DX$ ) for  $c$ -plane Zn-face and O-face epilayers at  $T = 4$  K.

one order of magnitude larger than for the O-face ones. For nitrogen concentrations over  $5 \times 10^{19} \text{ cm}^{-3}$  we were not able to observe any  $DX$  emission from the Zn-face layers and, thus, no data are provided in this range. This is explained by considering an increasing concentration of free holes which efficiently compensate the neutral donors and hence suppress their luminescence.

### C. Temperature- and power-dependent PL

The temperature dependence of the radiative optical transitions gives insights into the activation energies of the bound excitons which are required to, e.g., release electrons and holes from the donor and acceptor sites. Figure 5 shows the temperature dependence of the DAP band in the range from 8 to 200 K. The luminescence spectrum in the DAP range is rather independent of the temperature up to 100 K, whereas at higher temperatures the thermal quenching of the DAP band leads to an almost complete loss of the signal at 200 K. The linewidth of the zero-phonon line (ZPL) of the DAP band remains nearly constant, and no high energy broadening due to appearance of free-to-bound ( $e,A$ ) transitions is observed. However, a pronounced blueshift of the DAP band is visible with increasing temperature which is an indicator of weakly compensated material. In this case, donor-acceptor pairs with larger distance  $r$  (smaller Coulomb interaction) exhibit longer lifetimes and, thus, a higher probability for thermal dissociation. Hence, the fraction of close-distant pairs that contribute to the ensemble of radiative DAP recombinations increases with increasing temperature and the position of the DAP band gradually shifts to higher energies. For the samples with the highest acceptor concentrations a blueshift is not observed since the mean distance of the DAP is limited by the lattice sites and thus the DAP luminescence is dominated by close-distance pairs over the whole temperature range of Fig. 5.

Figure 6 displays power-dependent PL measurements for a  $c$ -plane Zn-face layer with a N concentration of  $6 \times 10^{19} \text{ cm}^{-3}$ . With increasing excitation density the DAP band

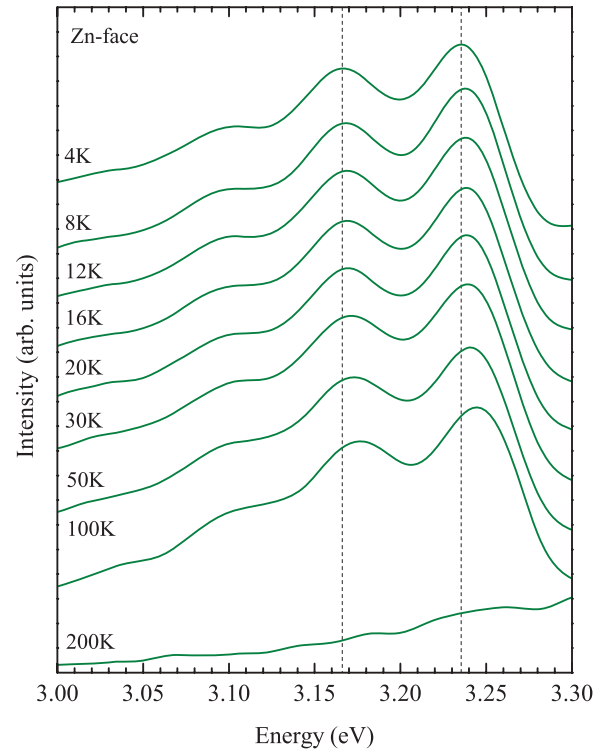


FIG. 5. (Color online) Temperature dependence of the DAP transition of a highly nitrogen-doped Zn-face epilayer.

shifts towards higher energies. This relation was previously explained by Thomas *et al.*<sup>45</sup> considering the Coulomb interaction between spatially located pairs at different distances with

$$h\nu = E_g - (E_A + E_D) + e^2/\epsilon r, \quad (1)$$

where  $h$ ,  $e$ , and  $\epsilon$  are the usual quantities,  $\nu$  is the photon frequency of the DAP luminescence,  $r$  the distance between the donor-acceptor-pairs,  $E_g$  the band gap of ZnO at the  $\Gamma$  point, and  $E_A$  and  $E_D$  are the acceptor and donor binding energies, respectively. The inset of Fig. 6 shows the energy position of the ZPL of the DAP band as function of the excitation density. With increasing excitation density, a blueshift of about 6 meV per order of magnitude occurs. This blueshift originates from the saturation of the distant long-lived pairs with comparatively small Coulomb interaction, and a redistribution to the short-lived closer pairs with larger Coulomb energy as follows from Eq. (1). It is noteworthy that this sample corresponds to the low-doping case where the potential fluctuations play a minor role since the ZPL of the DAP band is centered around 3.255 eV (see Figs. 2 and 3) and the blueshift with increasing excitation intensity is rather small. For higher acceptor doping levels the DAP band is redshifted, which can be understood within the framework of the fluctuating potentials model<sup>43</sup> by the local variation in the distribution of charged and neutral impurities as discussed below.

### D. Time-resolved PL measurements

We have investigated the recombination dynamics of several samples with nitrogen contents between  $2 \times 10^{19}$  and  $2 \times 10^{20} \text{ cm}^{-3}$ . The PL transients of the DAP band are shown in Fig. 7 for an equivalent continuous wave (cw)

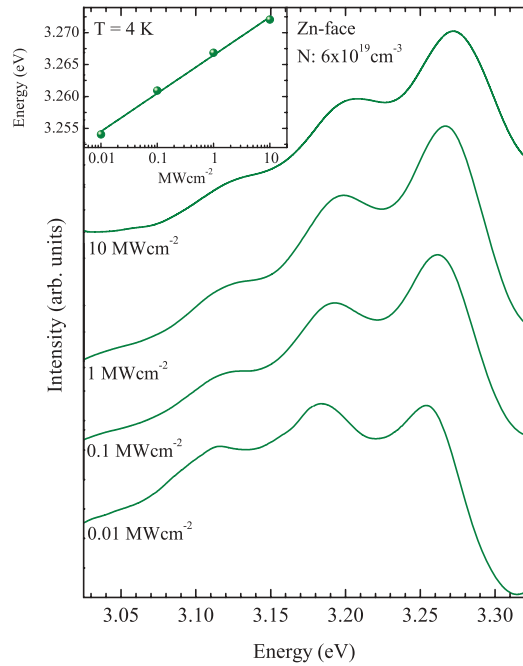


FIG. 6. (Color online) Power-dependent PL measurements of a Zn-face epilayer with a nitrogen content of  $6 \times 10^{19} \text{ cm}^{-3}$  at  $T = 4 \text{ K}$ . Inset: Shift of the zero-phonon line positions of the DAP recombination with increasing excitation power density.

excitation power of 1 mW at 10 K. All samples exhibit a pronounced nonexponential decay, which is typical for DAP transitions<sup>38,43,46</sup> and can be described by the model for distant donor-acceptor pairs developed by Thomas *et al.*<sup>45</sup> The radiative recombination probability of a DAP decreases with increasing distance between the donor and acceptor since the overlap between the electron and hole wave functions decreases for larger electron-hole distances. After laser excitation the initial fast decay arises from the closest DAPs followed by

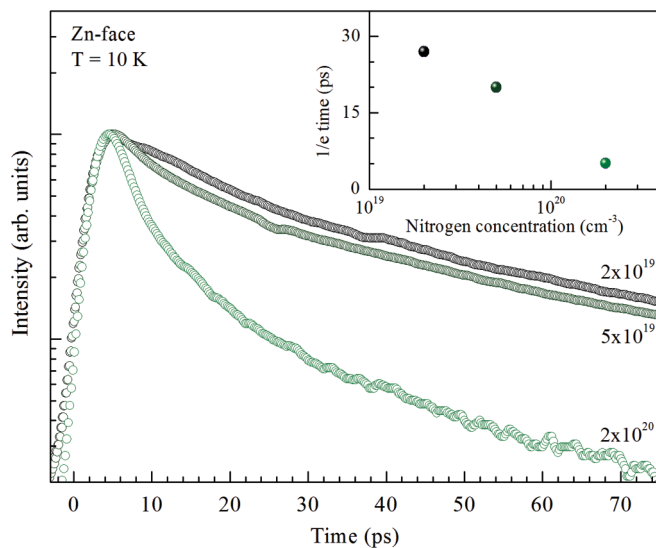


FIG. 7. (Color online) PL transients of the DAP transition of N-doped ZnO samples grown on Zn-face substrates with different N concentrations at 10 K. (Inset)  $1/e$  decay time for the closest donor-acceptor pairs as function of N concentration.

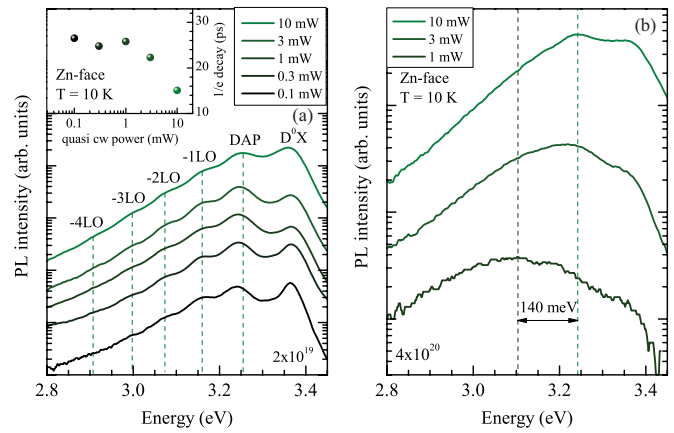


FIG. 8. (Color online) Excitation power-dependent PL measurements using pulsed fs excitation measured at 10 K. (a) N concentration  $2 \times 10^{19}$ ; (inset) decay times as function of excitation power; (b) N concentration  $4 \times 10^{20}$ .

gradually slower recombinations from more separated ones. With increasing nitrogen concentration, the decay dynamics become shorter as expressed by the  $1/e$  decay time as shown in the inset of Fig. 7. However, it should be noted that the  $1/e$  time does not provide a correct characterization of the entire nonexponential DAP decay dynamics but is sufficient for a qualitative analysis of the initial short decay which is determined by the closest DAP pairs and, thus, by the acceptor doping concentration. This decay time is about 30 ps for the sample with a nitrogen concentration of  $2 \times 10^{19} \text{ cm}^{-3}$  and decreases to about 5 ps for a nitrogen content of  $2 \times 10^{20} \text{ cm}^{-3}$ .

The PL spectra under pulsed-laser excitation for the samples doped with  $2 \times 10^{19}$  and  $4 \times 10^{20} \text{ cm}^{-3}$  for different power excitations are shown in Fig. 8. The corresponding lifetimes ( $1/e$ ) of the closest DAPs are plotted in the inset of Fig. 8. Apparently, higher excitation powers lead to smaller DAP lifetimes in accordance with the blueshift predicted by Eq. (1) which originates from the population of closer DAP states. The observed blueshift and broadening of the DAP transitions with increasing the excitation power density resembles the observation under cw excitation shown in Fig. 6 while the time-resolved results in Fig. 7 confirm the interpretation of the cw measurements.

#### IV. DISCUSSION

The change of the spectral shape of the DAP transition with increasing N-doping concentration (Figs. 2 and 3) and its modification by varying the excitation density (Figs. 6 and 8) is related to the high compensation in a highly doped system. As outlined for ZnSe:N, a wide band-gap semiconductor which shows close similarities to ZnO:N, the shallow donors and acceptors are ionized in highly compensated samples leading to internal electrical fields and to long-range potential fluctuations. The concentration of charged impurities is proportional to the amplitude and the length of the fluctuations. A theoretical model of the potential fluctuations in a highly compensated semiconductor has been introduced by Shklovskii and Efros.<sup>43</sup> It is able to successfully explain the compensation in ZnSe:N

and GaAs:Li and will now be applied to ZnO:N. In a highly compensated  $p$ -type semiconductor one can assume that the concentration of acceptors  $N_A$  is higher than the concentration of the residual compensating donors  $N_D$  which results in a hole concentration  $p = N_A - N_D$ . However, the high density of the charged donors and acceptors ( $N_{A^-}$ ,  $N_{D^+}$ ) will create a strong electrical field which leads to potential fluctuations of the valence and conduction bands and to spatially separated transitions between electrons and holes. The amplitude  $\gamma$  of the potential fluctuations depends on the concentration of charged impurities  $N_t = N_{A^-} + N_{D^+}$  and on the hole concentration  $p$  as expressed by Eq. (2) (Ref. 43):

$$\gamma = e^2/4\pi\epsilon\epsilon_0(N_t^{2/3}/p^{1/3}). \quad (2)$$

Hence, the recombination energy of the DAP transitions is modified if compared to Eq. (1) resulting in Eq. (3) (Ref. 43):

$$h\nu = E_g - (E_A + E_D) - 2\gamma. \quad (3)$$

Based on Eq. (2) it is apparent that the amplitude  $\gamma$  of the potential fluctuations increases with the increase of the charged impurity concentration  $N_t$ , but also increases with the decrease of the concentration of uncompensated free holes  $p$ . Equation (3) explains the origin of the PL band redshift in highly compensated samples. Furthermore, the long-range potential fluctuations lead to a broadening of the spatially indirect DAP transitions. By increasing the doping and thus also the compensation level, the amplitude of the potential fluctuations increases resulting in a broadening of the DAP ZPL line and its Logitudinal-Optical phonon replica and a shift of these bands to lower energies. Within this model it is clear that a varying excitation density has profound influence on the shape and line position of the DAP band. At the lowest excitation density, only a few donors and acceptors are occupied by photoexcited carriers which relax quickly to the lowest donor and the highest acceptor states. The DAP recombination process takes place between these lowest donors and highest acceptor states leading to the maximal redshift. At higher excitation densities when the photogenerated carrier concentration is high enough to screen the charged carriers, the flat band conditions are restored and the DAP band is at its usual position for lowly doped, lowly compensated samples.

The conclusions we can draw from the model of fluctuating potentials mainly concern the interplay between the number of free holes and the number of charged acceptors and donors ( $N_t$ ). The residual donor concentration  $N_D$  in the undoped films amounts to  $1 \times 10^{17} \text{ cm}^{-3}$ ; whether this number changes by doping with ammonia is not clear. We calculate the DAP shift  $2\gamma$  as a function of  $N_t$  ( $N_{A^-} + N_{D^+}$ ) for the two hole concentrations  $p = 5 \times 10^{15} \text{ cm}^{-3}$  and  $p = 1 \times 10^{17} \text{ cm}^{-3}$ . The experimentally observed shift of around 140 meV in Fig. 8(b) requires  $N_t$  around  $5 \times 10^{17} \text{ cm}^{-3}$  and  $2 \times 10^{18} \text{ cm}^{-3}$ , respectively (see Fig. 9). The amount of nitrogen in the films ( $< 4 \times 10^{20} \text{ cm}^{-3}$ ) does not equal the concentration of the shallow acceptors  $N_A$ , since the concentration of holes for an acceptor binding energy of 160 meV would otherwise substantially exceed  $N_D$  and compensation would be small thus resulting in the absence of potential fluctuations. It is more plausible that the hole concentration

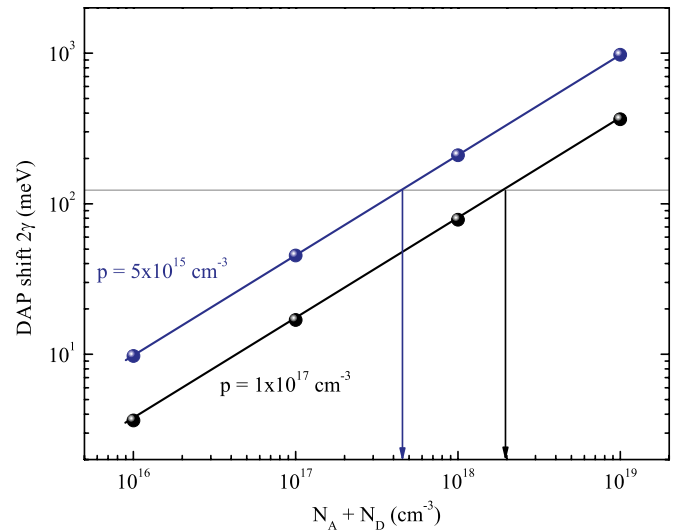


FIG. 9. (Color online) Energy shift of the DAP transition calculated within the model of fluctuating potentials for two hole concentrations as a function of the total impurity concentration.

$p$  is comparable or slightly above the value of  $N_D$ , which implies a more complicated model for the acceptor created by the ammonia doping. Maybe a complex acceptor model, such as is proposed in Ref. 37, could explain the behavior of nitrogen as an acceptor in ZnO. However, a detailed picture of the shallow nitrogen-related acceptor is still somehow speculative and cannot finally be deduced at this point. Nevertheless, the presented investigations presented here are conclusive concerning the role of the shallow acceptor states, which is directly reflected by the optical recombinations of ZnO to the shallow acceptor action in the optical recombinations of ZnO. It leaves no doubt that shallow acceptors are formed by ammonia doping, that they sufficiently compensate the shallow residual donors, and that they show all established properties of optical recombinations in weakly and highly acceptor-doped III-V and II-VI compound semiconductors.

## V. CONCLUSIONS

In conclusion, we have investigated the optical properties of neutral donor bound exciton ( $DX$ ) and donor-acceptor pair (DAP) transitions in a wide range of the nitrogen dopant concentration ( $10^{19}$ – $10^{21} \text{ cm}^{-3}$ ). We have grown doped epilayers up to a level where the DAP recombination dominates the radiative process. Such large dopant concentrations were achieved by growing homoepitaxial ZnO layers on nonpolar  $a$ -plane or polar Zn-face  $c$ -plane substrates, which favor the incorporation of nitrogen as an acceptor. This could not be achieved for the O-face  $c$ -plane substrates due to the higher incorporation of residual donors of this face. The comparison with other compound semiconductor materials leads to the conclusion that the samples change from lightly compensated to highly doped compensated, where fluctuating potentials have significant influence on the line position and spectral shape of the DAP band.

- <sup>1</sup>E. I. Rashba and G. E. Gurgenishvili, *Sov. Phys. Solid State* **4**, 759 (1962).
- <sup>2</sup>C. H. Park, S. B. Zhang, and S.-H. Wei, *Phys. Rev. B* **66**, 073202 (2002).
- <sup>3</sup>M. D. McCluskey and S. J. Jokela, *J. Appl. Phys.* **106**, 071101 (2009).
- <sup>4</sup>A. Janotti and C. G. Van de Walle Janotti, *Rep. Prog. Phys.* **72**, 126501 (2009).
- <sup>5</sup>A. Tsukazaki, A. Ohtomo, T. Onuma, M. T. Makino, M. Sumiya, K. Ohtani, S. F. Chichibu, S. Fuke, Y. Segawa, H. Ohno, H. Koinuma, and M. Kawasaki, *Nat. Mater.* **4**, 42 (2004).
- <sup>6</sup>D. C. Look and B. Claflin, *Phys. Status Solidi B* **241**, 624 (2004).
- <sup>7</sup>F. Zhuge, L. P. Zhu, Z. Z. Ye, D. W. Ma, J. G. Lu, J. Y. Huang, F. Z. Wang, Z. G. Ji, and S. B. Zhang, *Appl. Phys. Lett.* **87**, 092103 (2005).
- <sup>8</sup>T. Ohgaki, N. Ohashi, S. Sugimura, H. Ryoken, I. Sakaguchi, Y. Adachi, and H. Haneda, *J. Mater. Res. Rapid Commun.* **23**, 2293 (2008).
- <sup>9</sup>O. Bierwagen, T. Ive, C. G. Van de Walle, and J. S. Speck, *Appl. Phys. Lett.* **93**, 242108 (2008).
- <sup>10</sup>H. L. Mosbacker, Y. M. Strzhemechny, B. D. White, P. E. Smith, D. C. Look, D. C. Reynolds, C. W. Litton, and L. J. Brillson, *Appl. Phys. Lett.* **87**, 012102 (2005).
- <sup>11</sup>M. Schirra, R. Schneider, A. Reiser, G. M. Prinz, M. Feneberg, J. Biskupek, U. Kaiser, C. E. Krill, R. Sauer, and K. Thonke, *Physica B* **401**, 362 (2007).
- <sup>12</sup>M. R. Wagner, G. Callsen, J. S. Reparaz, J.-H. Schulze, R. Kirste, M. Cobet, I. A. Ostapenko, S. Rodt, C. Nenstiel, M. Kaiser, A. Hoffmann, A. V. Rodina, M. R. Phillips, S. Lautenschläger, S. Eisermann, and B. K. Meyer, *Phys. Rev. B* **84**, 035313 (2011).
- <sup>13</sup>K.-K. Kim, H.-S. Kim, D.-K. Hwang, J.-H. Lim, and S.-J. Park, *Appl. Phys. Lett.* **83**, 63 (2003).
- <sup>14</sup>Y. R. Ryu, T. S. Lee, and H. W. White, *Appl. Phys. Lett.* **83**, 87 (2003).
- <sup>15</sup>F. Reuss, C. Kirchner, Th. Gruber, R. Kling, S. Maschek, W. Limmer, A. Waag, and P. Ziemann, *J. Appl. Phys.* **95**, 3385 (2004).
- <sup>16</sup>M. Miyakawa, K. Ueda, and H. Hosono, *Nucl. Instrum. Methods Phys. Res., Sect. B* **191**, 173 (2002).
- <sup>17</sup>M. Schmidt, M. Ellguth, F. Schmidt, Th. Luder, H. v. Wenckstern, R. Pickenhain, M. Grundmann, G. Brauer, and W. Skorupa, *Phys. Status Solidi B* **247**, 1220 (2010).
- <sup>18</sup>B. T. Adekore, J. M. Pierce, R. F. Davis, D. W. Barlage, and J. F. Muth, *J. Appl. Phys.* **102**, 024908 (2007).
- <sup>19</sup>D. Stichtenoth, J. Dürr, C. Ronning, L. Wischmeier, and T. Voss, *J. Appl. Phys.* **103**, 083513 (2008).
- <sup>20</sup>D. C. Look, D. C. Reynolds, C. W. Litton, R. L. Jones, D. B. Eason, and G. Cantwell, *Appl. Phys. Lett.* **81**, 1830 (2002).
- <sup>21</sup>K. Iwata, P. Fons, A. Yamada, K. Matsubara, and S. Niki, *J. Cryst. Growth* **209**, 526 (2000).
- <sup>22</sup>A. B. M. A. Ashrafi, I. Suemune, H. Kumano, and S. Tanaka, *Jpn. J. Appl. Phys., Part 2* **41**, L1281 (2002).
- <sup>23</sup>A. Zeuner, H. Alves, J. Sann, W. Kriegseis, C. Neumann, D. M. Hofmann, B. K. Meyer, A. Hoffmann, U. Habocek, M. Straßburg, and A. Kaschner, *Phys. Status Solidi C* **1**, 731 (2004).
- <sup>24</sup>K. Minegishi, Y. Koiwai, Y. Kikuchi, K. Yano, M. Kasuga, and A. Shimizu, *Jpn. J. Appl. Phys., Part 2* **36**, L1453 (1997).
- <sup>25</sup>A. Krtschil, A. Dadgar, N. Oleynik, J. Bläsing, A. Diez, and A. Krost, *Appl. Phys. Lett.* **87**, 262105 (2005).
- <sup>26</sup>N. Haneche, A. Lussion, C. Sartel, A. Marzouki, V. Sallet, M. Oueslati, F. Jomard, and P. Galtier, *Phys. Status Solidi B* **247**, 1671 (2010).
- <sup>27</sup>K. Tamura, T. Makino, A. Tsukazaki, M. Sumiya, S. Fuke, T. Furumochi, M. Lippmaa, C. H. Chia, Y. Segawa, H. Koinuma, and M. Kawasaki, *Solid State Communications* **127**, 265 (2003).
- <sup>28</sup>M. Sumiya, A. Tsukazaki, S. Fuke, A. Othomo, H. Koinuma, and M. Kawasaki, *Appl. Surf. Sci.* **223**, 206 (2004).
- <sup>29</sup>A. Tsukazaki, M. Kubota, A. Othomo, T. Onuma, K. Ohtani, H. Ohno, S. F. Chichibu, and M. Kawasaki, *Jpn. J. Appl. Phys.* **44**, L643 (2005).
- <sup>30</sup>X.-L. Guo, H. Tabata, and T. Kawai, *J. Cryst. Growth* **237–239**, 544 (2002).
- <sup>31</sup>K. Thonke, Th. Gruber, N. Teofilov, R. Schönfelder, A. Waag, and R. Sauer, *Physica B* **308–310**, 945 (2001).
- <sup>32</sup>L. Wang and N. C. Giles, *Appl. Phys. Lett.* **84**, 3049 (2010).
- <sup>33</sup>S. Lautenschlaeger, S. Eisermann, M. N. Hofmann, U. Roemer, M. Pinnisch, A. Laufer, Bruno K. Meyer, H. v. Wenckstern, A. Lajn, F. Schmidt, M. Grundmann, J. Blaesing, and A. Krost, *J. Cryst. Growth* **312**, 2078 (2010).
- <sup>34</sup>S. Lautenschlaeger, J. Sann, N. Volbers, B. K. Meyer, A. Hoffmann, U. Habocek, and M. R. Wagner, *Phys. Rev. B* **77**, 144108 (2008).
- <sup>35</sup>M. R. Wagner, T. P. Bartel, R. Kirste, A. Hoffmann, J. Sann, S. Lautenschläger, B. K. Meyer, and C. Kisielowski, *Phys. Rev. B* **79**, 035307 (2009).
- <sup>36</sup>S. Lautenschlaeger, S. Eisermann, Bruno K. Meyer, G. Callsen, M. R. Wagner, and A. Hoffmann, *Phys. Status Solidi RRL* **3**, 16 (2009).
- <sup>37</sup>S. Lautenschlaeger, M. Hofmann, S. Eisermann, G. Haas, M. Pinnisch, A. Laufer, and B. K. Meyer, *Phys. Status Solidi B* **248**, 1217 (2011).
- <sup>38</sup>A. Zeuner, H. Alves, D. M. Hofmann, B. K. Meyer, A. Hoffmann, U. Habocek, M. Strassburg, and M. Dworzak, *Phys. Status Solidi B* **234**, R7 (2002).
- <sup>39</sup>B. K. Meyer, J. Sann, S. Lautenschläger, M. R. Wagner, and A. Hoffmann, *Phys. Rev. B* **76**, 184120 (2007).
- <sup>40</sup>E. Kurtz, S. Einfeldt, J. Nürnberger, S. Zerlauth, D. Hommel, and G. Landwehr, *Phys. Status Solidi B* **187**, 393 (1995).
- <sup>41</sup>H. P. Gislason, B. H. Yang, and M. Linnarsson, *Phys. Rev. B* **47**, 9418 (1993).
- <sup>42</sup>L. Eckey, U. v. Gfug, J. Holst, A. Hoffmann, A. Kaschner, H. Siegle, C. Thomsen, B. Schineller, K. Heime, M. Heuken, O. Schoen, and R. Beccard, *J. Appl. Phys.* **84**, 5828 (1998).
- <sup>43</sup>B. I. Shklovskii and A. L. Efros, *Electronic Properties of Doped Semiconductors* (Springer, Berlin, 1984), p. 52ff.
- <sup>44</sup>B. Hu, A. Yin, G. Karczewski, H. Luo, S. W. Short, N. Samarth, M. Dobrowolska, and J. K. Furdyna, *J. Appl. Phys.* **74**, 4153 (1993).
- <sup>45</sup>D. G. Thomas, J. J. Hopfield, and W. M. Augustyniak, *Phys. Rev.* **140**, 202 (1965).
- <sup>46</sup>C. Rauch, W. Gehlhoff, M. R. Wagner, E. Malguth, G. Callsen, R. Kirste, B. Salameh, A. Hoffmann, S. Polarz, Y. Aksu, and M. Driess, *J. Appl. Phys.* **107**, 024311 (2010).